IN-46-CR
1998
046 317

NASA/CR-97- 206692

Infrared Radiative Forcing and Atmospheric Lifetimes of Trace Species Based on Observations from UARS

K. Minschwaner, R. W. Carver
Department of Physics, New Mexico Institute of Mining and Technology, Socorro, New Mexico.

B. P. Briegleb
National Center for Atmospheric Research, Boulder, Colorado.

Abstract

Observations from instruments on the Upper Atmosphere Research Satellite (UARS) have been used to constrain calculations of infrared radiative forcing by CH_4, CCl_2F_2 and N_2O, and to determine lifetimes of CCl_2F_2 and N_2O. Radiative forcing is calculated as a change in net infrared flux at the tropopause that results from an increase in trace gas amount from pre-industrial (1750) to contemporary (1992) times. Latitudinal and seasonal variations are considered explicitly, using distributions of trace gases and temperature in the stratosphere from UARS measurements and seasonally averaged cloud statistics from the International Satellite Cloud Climatology Project. Top-of-atmosphere fluxes calculated for the contemporary period are in good agreement with satellite measurements from the Earth Radiation Budget Experiment. Globally averaged values of the radiative forcing are 0.536, 0.125, and 0.108 W m^{-2} for CH_4, CCl_2F_2, and N_2O, respectively. The largest forcing occurs near subtropical latitudes during summer, predominantly as a result of the combination of cloud-free skies and a high, cold tropopause. Clouds are found to play a significant role in regulating infrared forcing, reducing the magnitude of the forcing by 30-40% compared to the case of clear skies. The vertical profile of CCl_2F_2 is important in determining its radiative forcing; use of a height-independent mixing ratio in the stratosphere leads to an overprediction of the forcing by 10%. The impact of stratospheric profiles on radiative forcing by CH_4 and N_2O is less than 2%. UARS-based distributions of CCl_2F_2 and N_2O are used also to determine global destruction rates and instantaneous lifetimes of these gases. Rates of photolytic destruction in the stratosphere are calculated using solar ultraviolet irradiances measured on UARS and a line-by-line model of absorption in the oxygen Schumann-Runge bands. Lifetimes are 114 ± 22 and 118 ± 25 years for CCl_2F_2 and N_2O, respectively.

Introduction

Increases in the atmospheric abundances of CH_4, CCl_2F_2 (CFC-12) and N_2O from the pre-industrial to the present time have had a significant effect on the radiative and photochemical state of the atmosphere. The enhanced infrared opacity as a result of these changes accounts for nearly one-third of the total, post-industrial radiative forcing [*Intergovernmental Panel on Climate Change* (IPCC), 1995]. In addition, CH_4, CCl_2F_2, and N_2O are significant sources of hydrogen, chlorine, and nitrogen radicals in the stratosphere, and thus play an important role in the budget of stratospheric ozone. Global destruction rates of CCl_2F_2 and N_2O are determined primarily by ultraviolet photolysis in the stratosphere.

Although the longwave effects of trace gas increases were recognized some time ago [*Ramanathan*, 1975; *Wang et al.*, 1976], it is only recently that global distributions have become available for including latitudinal as well as seasonal effects. Calculations of radiative forcing have, for the most part, been based on results using typical midlatitude vertical profiles of temperature, water vapor, and ozone [*Wang et al.*, 1980; *Hansen et al.*, 1981; *Ramanathan et al.*, 1987]. The computed flux, however, may not be identical to the global average of separate calculations at each latitude (see, for example, Chapter 7 of *World Meteorological Organization* (WMO) [1991]; *Pinnock et al.* [1995]). Furthermore, the decrease in concentrations of CH_4, CCl_2F_2, and N_2O with increasing altitude above the tropopause can influence the downward flux at the tropopause level, thereby impacting the radiative forcing [*Ramanathan et al.*, 1985]. These effects are accounted for implicitly within the context of two- and three-dimensional model studies [*Kiehl and Briegleb*, 1993; *Hauglustaine et al.*, 1994; *Hansen et al.*, 1997], with trace gas distributions determined internally by the model.

The importance of CH_4, N_2O, most CFC's to the Earth's longwave radiation budget follows from the spectral location of the principal IR bands involved. Most are located within the relatively transparent spectral window between 8 and 12 μm. The accurate specification of stratospheric ozone in the radiative calculations is thus important due to the presence of the O_3 9.6 μm band. Equally important, tropospheric clouds are strong sources of opacity in the 8-12 μm window, and the proper representation of clouds is critical to the evaluation of radiative forcing at the tropopause. High clouds in the troposphere have been shown to exert a strong influence on the stratospheric IR heating by ozone [*Dessler et al.*, 1996], as well as the radiative forcing by tropospheric O_3 [*Forster et al.*, 1995] and CFC replacements [*Pinnock et al.*, 1995].

The destruction of N_2O and CCl_2F_2 is thought to take place primarily in the stratosphere. Most of the loss occurs through photodissociation by absorption of solar ultraviolet radiation in the 190 to 220 nm spectral region, at altitudes between 20 and 40 km [*Minschwaner et al.*, 1993]. Lifetimes for N_2O and CFC compounds have been estimated using two-dimensional photochemical models of the middle atmosphere [e.g., *Ko and Sze*, 1982], with calculated values determined by the balance between stratospheric loss and influx to the stratosphere by cross-tropopause transport in the tropics. A more empirical method applies calculated destruction rates to observed distributions in the stratosphere [*Johnston et al.*, 1979]. If the source terms are accurately known, then the lifetime can also be estimated from the total atmospheric burden [e.g., *Kaye et al.*, 1994]. A novel technique outlined by *Plumb and Ko* [1992] employs correlations between long-lived tracers in the stratosphere to determine lifetime ratios. The use of this technique is discussed within the framework of three-dimensional model calculations by *Avallone and Prather* [1997], and is applied to ER-2 observations in stratosphere by *Volk et al.* [1997].

The present study is motivated by the availability of global-scale observations from the Upper Atmosphere Research Satellite (UARS) which are relevant to the evaluation of radiative forcings and lifetimes of trace gases. UARS measurements of CH_4, CCl_2F_2, N_2O, O_3, H_2O, temperature, and solar ultraviolet irradiances are used to represent the physical and chemical state of the contemporary stratosphere. Complementary measurements of trace gas mixing ratios at the surface, mean cloud statistics from the International Satellite Cloud Climatology Project (ISCCP), and average longwave fluxes from the Earth Radiation Budget Experiment (ERBE) are used to complete this picture. The goal is to take advantage of the unprecedented spatial and temporal coverage of the UARS measurements and apply them to the evaluation of radiative forcing by CH_4, CCl_2F_2, and N_2O, and to determine atmospheric lifetimes for CCl_2F_2 and N_2O.

UARS Distributions of Trace Gases and Temperature

Climatological distributions of trace gases were constructed from zonal averages of UARS observations over 2-month periods bracketing the equinoxes and solstices. The total time interval extends from March 1992 to January 1993. All calculations were carried out a 5° latitude grid from 77.5°S to 77.5°N. Constant values were used poleward of 77.5° for the purposes of obtaining global averages. Vertical levels were spaced 100 mb apart in the troposphere, decreasing to 10-20 mb near the tropopause and lower stratosphere. Vertical resolution in the middle and upper stratosphere was approximately 3 km.

Distributions of CH_4, CCl_2F_2, and N_2O in the stratosphere were derived from vertical profiles measured by the Cryogen Limb Array Etalon Spectrometer (CLAES) onboard UARS. The CLAES instrument observed limb emission in vibration-rotation spectra between 3.5 and 15 μm for retrieval of trace gas mixing ratios, pressure, and temperature [*Roche et al.*, 1993]. Version 7, level 3AT data were used for all three gases. Averages for each latitude bin were obtained by weighting all values according to the data quality indicator associated with each point. The zonally averaged vertical profile was linearly interpolated from the UARS standard pressure levels to our adopted vertical grid. CLAES data were used from 0.1 mb down to 46 mb; values below this level were determined using a cubic spline interpolation to the tropopause (specification of the tropopause pressure is discussed below).

Mixing ratios in the troposphere, assumed to be height independent due to mixing, were obtained from 1991-92 measurements from the surface network operated by the Climate Monitoring and Diagnostics Laboratory for CH_4 [*Tans et al.*, 1992], and for CCl_2F_2 and N_2O [*Montzka et al.*, 1992]. We approximated latitudinal gradients in mixing ratios using linear fits to data from six surface stations ranging from 82.5°N to 40.7°S. This variation is small for N_2O (less than 1% from pole-to-pole), but is significant for CH_4 (~9% pole-to-pole) and CCl_2F_2 (~6%).

Other model inputs which are constrained by data from UARS include stratospheric O_3 and H_2O. Correct specification of ozone is of some importance for the infrared flux due to spectral overlaps in the wings of the O_3 9.6 μm band and the N_2O 7.8 μm band, the CH_4 7.7 μm band, and CCl_2F_2 absorption bands near 9 μm. The 6.7 μm band of water has an effect also on the N_2O and CH_4 bands. In the ultraviolet, the short-wavelength tail of the ozone Hartley band contributes significantly to the opacity near 200 nm, and therefore impacts photodissociation of both CCl_2F_2 and N_2O. Zonally averaged distributions of O_3 and H_2O were compiled based on measurements from the UARS Microwave Limb Sounder (MLS), which observes limb emission at millimeter wavelengths [*Waters* 1993; *Froidevaux et al.*, 1994]. Version 3, level 3AT data from the 205-GHz radiometer was used for O_3; data from the 183-GHz radiometer was used for H_2O. Zonal and seasonal averages of MLS measurements above 50 mb were constructed in a manner similar to the CLAES data described above. Ozone in the troposphere was based on climatological values from *Oltmans* [1981] and *Levy* [1985]. Tropospheric water vapor was specified on the basis of standard AFGL models [*Anderson et al.*, 1985] with values interpolated in season and latitude.

The vertical profile of temperature is another important parameter in the calculation of infrared forcing. Temperatures in the upper atmosphere have an impact also on ultraviolet photolysis through the temperature dependence of absorption cross sections, most notably in the O_2 Schumann-Runge (S-R) bands, with a corresponding effect on the the penetration of ultraviolet radiation to the middle and lower stratosphere. Temperatures were adopted from the National Meteorological Center (NMC) analysis [*McPherson et al.*, 1979] which are included as correlative data in the UARS data distribution. NMC temperatures were averaged over season and latitudes, similar to the CLAES trace gas data, from the surface to 70 mb. CLAES measurements of temperature were adopted above 70 mb. We found that a climatological tropopause could be identified, for each season, by fitting the temperature minimum in the NMC data with functions of the form

$$P_T = A - B \exp\left[-(\phi/C)^4\right] \qquad (1)$$

where P_T is the tropopause pressure, ϕ is latitude, and A, B, and C are fitting constants.

Distributions of CH_4, CCl_2F_2, N_2O, and O_3 for the September-October, 1992 time period are shown in Figure 1. The dashed horizontal lines indicate the pressure level which divides UARS-based distributions from the region of interpolation. The tropopause pressure is shown by the bottom dashed curve in each figure. Of particular importance for our calculations are the decreases in mixing ratios of CH_4, CCl_2F_2, and N_2O in the stratosphere as well as latitudinal variations in vertical profiles. Distributions of H_2O and temperature for the same time period are shown in Figure 2, along with the distributions of cloud fraction and heights assumed in the calculations. These are derived from averages over the 1983-1990 time period for low, middle, and high cloud fractions from the International Satellite Cloud Climatology Project (ISCCP) [*Rossow and Schiffer*, 1991]. Low clouds are assumed to be located between 850 and 750 mb, independent of latitude. Middle-level clouds are placed in a 100-mb thick layer centered near 500 mb at mid and high latitudes, and near 550 mb in tropics, as shown in Figure 2. High clouds are located in a 20-mb thick layer located just below the tropopause.

Radiative Calculations

As discussed by *IPCC* [1995], the concept of radiative forcing is a valuable measure of the first-order climatic impact of a greenhouse gas. The forcing is defined by the change in net infrared flux at the tropopause due to a prescribed change in greenhouse gas amount, holding all other model parameters fixed (except for stratospheric temperatures, as discussed below). Adoption of the tropopause as a reference is motivated by the fact that a change in radiative flux at this level appropriately expresses the radiative forcing of the climate system as a whole, since the surface and troposphere are a tightly coupled thermodynamic system. In addition, defining the forcing in terms of the radiative flux change avoids uncertainties associated with a given climate response, for example surface temperature, which depends on sensitivities and feedbacks that are evidently model-dependent (e.g., *IPCC* [1990]). However, care must be taken to account for the temperature response in the stratosphere [*Hansen et al.*, 1981; *Ramanathan*, 1987]. By maintaining radiative equilibrium (or constant heating/cooling) in the stratosphere, any change in flux at the tropopause is then the same as at the top of the atmosphere (TOA).

Infrared fluxes were calculated using a longwave band model developed at the National Center for Atmospheric Research. This is a 100 cm^{-1} band model which includes infrared opacity by H_2O, CO_2, and O_3, and considers also the major absorption bands of CH_4, N_2O, CFC-11, and CFC-12 (similar to the CCM2 radiation code described by *Briegleb* [1992]). Net longwave fluxes calculated with this model agree with detailed line-by-line calculations to within 1% [*Briegleb*, 1992]. We have, in addition, compared results for flux changes induced by changes in CH_4 and N_2O with line-by-line calculations by *Clough and Iacono* [1995]. Results at the tropopause agree to within 10%.

Figures 3a and 3b compare the TOA flux calculated with the model with measurements from the Earth Radiation Budget Experiment (ERBE) [*Barkstrom*, 1984] averaged over the 1985-1988 period. The agreement is within the uncertainties in flux (± 5 W/m^2) for nearly all latitudes and seasons. Results for June-July (Fig. 3a) clearly show the impact of high clouds in the intertropical convergence zone between 5° and 10°N which give rise to a minimum in TOA flux. This minimum shifts to south of the equator in both the ERBE observations and model calculations for December-January (Fig. 3b). Calculated TOA fluxes are sensitive to assumptions of cloud liquid water paths (lwp) and effective drop radii (r_e) assumed in the model. We adopted values for the three cloud types that are consistent with measurements [*Stephens*, 1978; *Stephens and Platt*, 1987]; these are identical to the values used by *Dessler et al.* [1996] (lwp = 125, 75, 15 g/m^2, r_e = 10, 11, 18 μm, for low, middle, and high clouds, respectively). Surface emissivity was fixed at 0.85, independent of latitude and season. Comparison of model shortwave albedo with ERBE averages (not shown) also indicated a very good level of agreement.

For the determination of instantaneous lifetimes, photochemical loss due to ultraviolet photodissociation was calculated using the high-resolution radiation code described by *Minschwaner et al.* [1993]. Solar irradiances above the atmosphere were specified according to measurements from the Solar-Stellar Irradiance Comparison Experiment (SOLSTICE) onboard UARS, averaged over the month of March, 1992. These are high resolution (0.1 nm) measurements of the full-disk, solar spectral irradiance between 115 and 420 nm [*Rottman et al.*, 1993]. Calibration is maintained to within 1% using a collection of bright blue stars as radiance standards [*Woods et al.*, 1993]. Version 7, level 3BS irradiances with a spectral resolution of 1 nm were used over the full spectral range. Oxygen cross sections in the S-R band region followed the line-by-line analysis by *Minschwaner et al.* [1992]. Cross sections for the O_2 Herzberg continuum were adopted from *Yoshino et al.* [1988], and for O_3, CCl_2F_2, and N_2O from *DeMore et al.* [1994]. Below 205 nm, solar irradiances and all cross sections other than O_2 were linearly interpolated to the high resolution (0.002 nm) spectral grid necessary to capture the rotational structure in O_2 S-R band absorption. Effects of scattering above 190 nm were included based on the formulation of *Meier et al.* [1982].

The instantaneous lifetime for each gas was determined from the ratio of its 1992 global inventory, M, by the calculated global removal rate, L:

$$\tau(1992) = M/L \tag{2}$$

The two quantities in the above equations are defined by

$$M = 2\pi R_e^2 \int dz \int n(\phi, z, 1992) cos\phi d\phi \tag{3}$$

$$L = 2\pi R_e^2 \int dt \int dz \int n(\phi, z, t) J(\phi, z, t) cos\phi d\phi \tag{4}$$

where $n(\phi, z, t)$ is the local concentration at latitude ϕ, altitude z, and time t, and where R_e is the Earth's radius. The corresponding loss frequency, J, is set primarily by photodissociation, although total loss includes a small contribution ($5-10\%$) due to reaction with $O(^1D)$.

Results

Radiative Forcing

The radiative forcing from pre-industrial (1750) to the 1992 time period was calculated using pre-industrial mixing ratios of 700 ppb CH_4, 0 ppt CCl_2F_2, and 275 ppb N_2O in the troposphere [*IPCC*, 1995]. Except for CCl_2F_2, there are no corresponding estimates for stratospheric distributions. A reasonable approximation, however, is to assume the same relative distribution as is currently observed. This follows from the fact that the stratospheric loss scales linearly with trace gas amount. Therefore, pre-industrial trace gas distributions were estimated by scaling all vertical profiles according to the ratio of pre-industrial to present-day mixing ratios in the troposphere.

The model was modified for the study of radiative forcing by allowing stratospheric temperatures to adjust so that stratospheric heating/cooling rates were the identical to values calculated for the pre-industrial stratosphere. This approach essentially assumes a fixed dynamical heating/cooling in the stratosphere rather than complete radiative equilibrium, but the final results should be comparable [*Ramanathan and Dickinson*, 1979]. Temperatures were adjusted iteratively until the net heating rate changed by less than 5×10^{-4} K/day at all levels above the tropopause.

The magnitude of radiative forcing for CH_4, CCl_2F_2, and N_2O as a function of season and latitude is shown in Figure 4. Values are largest in the summer subtropics, consistent with a relatively warm surface, cold tropopause, and comparatively clear skies. A similar behavior was noted in the 3-D simulations by *Kiehl and Briegleb* [1993]. Latitudinal differences in the forcing vary by up to a factor of 3 between the tropics and high latitudes in the winter hemisphere. Also included in Figure 4 is the assumed distribution of high cloud as a function of season and latitude. The patterns indicate a high degree of anticorrelation between high cloud fraction and the magnitude of radiative forcing for all three gases. These results are consistent with variations with respect to latitude (primarily vertical profiles of temperature) and cloud cover found for HFC radiative forcings by *Pinnock et al.* [1995].

Globally-averaged values of radiative forcing are listed in Table 1, along with results from the 42°N summer calculation and values reported in *IPCC* [1995]. Our results imply that the use of a midlatitude summer atmosphere to represent the global average forcing results in an overprediction of about 5% for all three gases. Differences between the UARS-based forcings and *IPCC* [1995] values are +14%, −11%, and −23% for CH_4, CCl_2F_2, and N_2O, respectively. These discrepancies are within uncertainties (15%) associated with *IPCC* forcings for CH_4 and CCl_2F_2, but the difference for N_2O could be significant. The treatment of clouds may play a role; the clear-sky forcing at midlatitudes increases to 0.143 W/m^2 (see below). However, a systematic difference in cloud fractions or radiative properties would be expected to have the same sign for all three gases. Use of a midlatitude summer atmosphere with clouds only partially improves the agreement.

Sensitivities of calculated forcing clouds and to vertical profiles of mixing ratio in the stratosphere are summarized in Table 2. As expected, forcings are larger for clear skies because absorbing gases at the tropopause and in the lower stratosphere see a warmer effective temperature below, leading to an enhanced greenhouse influence. Differences range between 28 to 36% at midlatitudes and are even more pronounced in tropics. The latter result arises due to the higher contrast in temperature between cloud top and the lower troposphere in the tropics as compared to midlatitudes. Midlatitude cloud effects are similar to the 36% clear-sky enhancement for CCl_3F forcing at midlatitudes presented by *Pinnock et al.* [1995].

The impact of using realistic stratospheric profiles was discussed by *Ramanathan et al.* [1985] for CH_4 and N_2O, and more recently by *Hanson et al.* [1997] and *Christidis et al.* [1997] for CFCs and HCFCs. However, previous studies either assumed exponential decreases using a constant scale height, or used model-calculated profiles instead of observed distributions. Our calculations show a negligible impact on CH_4 and N_2O (Table 2) which is consistent with the results of *Ramanathan et al.* [1985]. On the other hand, the forcing for CCl_2F_2 is increased by up to 10% if a uniform mixing ratio is used. The reason for the different behavior for CCl_2F_2 lies in the fact that the pre-industrial atmosphere contained no CCl_2F_2. There is clearly a difference in net flux between assumption of a uniform mixing ratio and one that decreases in the stratosphere for all three gases. However, with the scaling procedures used here to approximate CH_4 and N_2O mixing ratios in the pre-industrial stratosphere, this flux difference appears in both the pre-industrial as well as the contemporary cases, and very nearly cancels out in the radiative forcing. This is not true for CCl_2F_2, which has a zero (uniform in altitude) profile in the pre-industrial case.

Lifetimes for CCl_2F_2 and N_2O

Instantaneous lifetimes were calculated using the sum of global loss rates for the four separate seasons (equation 4), and the mean atmospheric burden during the same period (equation 3). Lifetimes for CCl_2F_2 and N_2O are 114 $\pm$22 and 118 $\pm$25 years, respectively. Uncertainties are estimated based on the standard deviation of the CLAES zonal means where loss rates are a maximum (12% for CCl_2F_2 and 9% for N_2O), uncertainty in actinic flux (5% in solar irradiance and 10% in atmospheric transmission), and absorption cross section uncertainties (10% for CCl_2F_2 and 15% for N_2O).

Calculated rates for stratospheric loss were largest in the tropical mid-stratosphere. Globally integrated rates were found to be moderately dependent on season; removal rates were 12% larger during the equinoxes as compared to the solstices. These higher rates are a consequence of smaller solar zenith angles in the tropics during the equinoxes, with associated increases in actinic fluxes in the lower stratosphere.

Previous estimates of the CCl_2F_2 lifetime range from 95 years [*Ko et al.*, 1991] to 180 years [*Cunnold et al.*, 1994]; the range for N_2O is 110 years [*Ko et al.*, 1991] to 182 years [*Golombek and Prinn*, 1986]. Our results favor the lower end of these ranges and are in good agreement with previous instantaneous lifetimes, 116 years for CCl_2F_2, 123 years for N_2O, obtained by *Minschwaner et al.* [1993]. The latter estimates were obtained using the same empirical technique and nearly identical calculations for photochemical loss as used here; however the level of agreement is somewhat surprising in view of the fact that the trace gas distributions used by *Minschwaner et al.* were based on a relatively sparse collection of balloon and aircraft data.

The steady-state lifetime, where emissions to the atmosphere exactly balance photochemical loss, are generally shorter than the instantaneous lifetime for gases whose concentrations are increasing with time. The difference arises from the time lag between temporal changes in abundances for the stratosphere relative to the troposphere. The distinction between steady-state and instantaneous lifetime is small for N_2O because the growth rate of about 0.25% yr^{-1} *Montzka et al.*, 1992] does not significantly impact stratospheric/tropospheric abundances over timescales relevant for the turnover of stratospheric air (less than 5 years [*Rosenlof and Holton*, 1993]). However, the mean growth rate for CCl_2F_2 is much larger, averaging about 3.5% yr^{-1} between 1988 and 1992 [*Elkins et al.*, 1993]. Assuming a mean age of between 2 to 4 years for mid-stratosphere air in the tropics [*Hall and Plumb*, 1994; *Boering et al.*, 1996], and an instantaneous lifetime of 114 years, the estimated steady-state lifetime for CCl_2F_2 is between 99 and 106 years. Including the uncertainty in instantaneous lifetimes yields steady-state lifetimes of 103 $\pm$25 years for CCl_2F_2, and 117 $\pm$26 years for N_2O.

Steady-state lifetimes of 102 and 120 years for CCl_2F_2 and N_2O, respectively, are presented by *IPCC* [1995]. These lifetimes, based primarily on results of 2-D model calculations, are in very good agreement with our UARS-based values. Results from the GISS/UCI three-dimensional chemical transport model (CTM) yield steady-state lifetimes of 90 and 113 years for CCl_2F_2 and N_2O, respectively [*Avallone and Prather*, 1997] which are somewhat shorter than calculated here but within the range of uncertainty. As noted by *Avallone and Prather*, there may be a tendency in the CTM for excessive vertical mixing in the tropical stratosphere, leading to enhanced rates of calculated destruction. The use of observed tracer correlations by *Volk et al.* [1997] indicates lifetimes of 87 and 122 years for CCl_2F_2 and N_2O, respectively. These are also consistent with our results, although the CCl_2F_2 steady-state lifetime is near the low range of the UARS-based value.

Concluding Remarks

Our radiative calculations constrained by UARS and ISCCP observations imply a total post-industrial forcing of 0.77 W m^{-2} due to increasing burdens of trace gases CH_4, CCl_2F_2, and N_2O. For comparison, the estimated CO_2-induced forcing is 1.56 W m^{-2} over the same period [*IPCC*, 1995]. Equally important, our results indicate a strong dependence on trace gas forcing on season and latitude. Cloud effects, particularly the fraction of high clouds in the tropics, play a significant role in regulating the radiative forcing. In this regard it is important to note that even small changes in cloud amount could be just as important as changes in trace gas abundances.

The radiative forcing and atmospheric lifetime both enter into the evaluation of the global warming potential (GWP) of a greenhouse gas. The GWP is defined as the time-integrated radiative forcing from the instantaneous release of 1 kg of trace gas, expressed relative to that from 1 kg of CO_2 [*IPCC*, 1990]. For the trace species considered here, the magnitudes of post-industrial radiative forcings and atmospheric lifetimes are broadly similar to currently accepted values, implying GWP's which are consistent with results presented in *IPCC* [1995]. However, our radiative forcing by N_2O is 23% smaller in magnitude and our steady-state lifetime is about 2% shorter; taken together these results suggests that the N_2O GWP may be about 25% less than the currently recommended value.

Acknowledgments. This research was supported by UARS Guest Investigator grant #NAG 5-2847 from NASA's Mission to Planet Earth Program. The National Center for Atmospheric Research is sponsored by the National Science Foundation. We thank Guy Brasseur, David Edwards, and Keith Shine for useful comments and discussions, and Michael Iacono for providing results of line-by-line radiative calculations. UARS data was obtained from the NASA GFSC Distributed Active Archive Center, and from CD-ROMs made available by NASA GSFC.

References

Anderson, G. P., S. A. Clough, F. X. Kneizys, J. H. Chetwynd, and E. P. Shettle, AFGL atmospheric constituent profiles (0-120km), *AFGL Tech. Rep., AFGL-TR-86-0110*, 43 pp., Air Force Phillips Lab., Hansom AFB, Mass., 1986.

Avallone, L. M., and M. J. Prather, Tracer-tracer correlations: Three-dimensional model simulations and comparisons to observations, *J. Geophys. Res., 102*, 19,233-19,246, 1997.

Barkstrom, B. R., The Earth Radiation Budget Experiment (ERBE), *Bull. Am. Meteorol. Soc., 65*, 1170-1185, 1984.

Briegleb, B. P., Longwave band model for thermal radiation in climate studies, *J. Geophys. Res.*, 97, 11,475-11,485, 1992.

Christidis, N., M. D. Hurley, S. Pinnock, K. P. Shine, and T. J. Wallington, Radiative forcing of climate change by CFC-11 and possible CFC replacements, *J. Geophys. Res., 102*, 19,597-19,609, 1997.

Cunnold, D. M., P. J. Fraser, R. F. Weiss, R. G. Prinn, P. G. Simmonds, B. R. Miller, F. N. Alyea, and A. J. Crawford, Global trends and annual releases of $CFCl_3$ and CF_2Cl_2 estimated from ALE/GAGE and other measurements from July 1978 to June 1991, *J. Geophys. Res., 99*, 1107-1126, 1994.

DeMore, W. B., S. P. Sander, D. M. Golden, R. F. Hampson, M. J. Kurylo, C. J. Howard, A. R. Ravishankara, C. E. Kolb, and M. J. Molina, Chemical kinetics and photochemical data for use in stratospheric modeling, Evaluation 11, *JPL Pub. 94-26*, Jet Propul. Lab., Pasadena, Calif., 1994.

Dessler, A. E., K. Minschwaner, E. M. Weinstock, E. J. Hintsa, J. G. Anderson, and J. M. Russell, III, The effects of tropical cirrus clouds on the abundance of lower stratospheric ozone, *J. Atmos. Chem., 23*, 209-220, 1996.

Elkins, J. W., T. M. Thompson, T. H. Swanson, J. H. Butler, B. D. Hall, S. O. Cummings, D. A. Fisher, and A. G. Raffo, Decrease in the growth rates of atmospheric chlorofluorocarbons 11 and 12, *Nature, 364*, 780-783, 1993.

Forster, P. M. de F., C. E. Johnson, K. S. Shaw, J. A. Pyle, and K. P. Shine, Further estimates of radiative forcing due to tropospheric ozone changes, *Geophys. Res. Lett., 23*, 3321-3324, 1996.

Froidevaux, L., J. W. Waters, W. G. Read, L. S. Elson, D. A. Flower, and R. F. Jarnot, Global ozone observations from the UARS MLS: An overview of zonal-mean results, *J. Atmos. Sci., 51*, 2846-2866, 1994.

Golombek, A., and R. G. Prinn, A global three-dimensional model of the circulation and chemistry of $CFCl_3$, CF_2Cl_2, CH_3CCl_3, CCl_4, and N_2O, *J. Geophys. Res., 91*, 3985-4001, 1986.

Hansen, J., D. Johnson, A. Lacis, S. Lebedeff, P. Lee, D. Rind, and G. Russell, Climate impact of increasing atmospheric carbon dioxide, *Science, 213*, 957-966, 1981.

Hansen, J., M. Sato, and R. Ruedy, Radiative forcing and climate response, *J. Geiphys. Res., 102*, 6831-6864, 1997.

Hauglustaine, D. A., C. Granier, G. P. Brasseur, and G. Megie, The importance of atmospheric chemistry in the calculation of radiative forcing on the climate system, *J. Geophys. Res., 99*, 1173-1186, 1994.

Cloug, S. A., and M. J. Iacono, Line-by-line calculation of atmospheric fluxes and cooling rates 2. Application to carbon dioxide, ozone, methane, nitrous oxide and the halocarbons, *J. Geophys. Res., 100*, 16,519-16,535, 1995.

Intergovernmental Panel on Climate Change, *Climate Change: The IPCC Scientific Assessment*, edited by J. T. Houghton, C. J. Jenkins, and J. J. Ephraums, 365 pp., Cambridge University Press, New York, 1990.

Intergovernmental Panel on Climate Change, *Climate Change 1994, Radiative Forcing of Climate Change and An Evaluation of the IPCC IS92 Emission Scenarios*, 339 pp., Cambridge University Press, New York, 1995.

Johnston, H. S., O. Serang, and J. Podolske, Instantaneous global nitrous oxide photochemical rates, *J. Geophys. Res.*, 84, 5077-5082, 1979.

Kaye, J., S. Penkett, and F. Ormond, *Concentrations, Lifetimes, and Trends of CFCs, Halons, and Related Species*, NASA Ref. Publ. 1339, NASA Office of Mission to Planet Earth, Science Division, Washington DC.

Kiehl, J. T., and B. P. Briegleb, The relative roles of sulfate aerosol and greenhouse gases in climate forcing, *Science, 260*, 311-314, 1993.

Ko, M. K. W., and N. D. Sze, A 2-D model calculation of atmospheric lifetimes for N_2O, CFC-11 and CFC-12, *Nature, 297*, 317-319, 1982.

Ko, M. K. W., N. D. Sze, and D. K. Weisenstein, Use of satellite data to constrain the model-calculated atmospheric lifetime of N_2O: implications for other trace gases, *J. Geophys. Res., 96*, 7547-7552, 1991.

Levy, H., II, J. D. Mahlman, W. J. Moxim, and S. C. Liu, Tropospheric ozone: The role of transport, *J. Geophys. Res., 90*, 3753-3772, 1985.

McPherson, R., D., K. H. Bergman, R. E. Kistler, G. E. Rasch, and D. S. Gordon, The NMC operational global data assimilation system, *Mon. Wea. Rev., 107*, 1445-1461, 1979.

Meier, R. R., D. E. Anderson, and M. Nicolet, Radiation field in the troposphere and stratosphere from 240-1000 nm I. General analysis, *Planet Space Sci., 30*, 923-933, 1982.

Minschwaner, K., G. P. Anderson, L. A. Hall, and K. Yoshino, Polynomial coefficients for calculating O_2 Schumann-Runge cross sections at 0.5 cm^{-1} resolution, *J. Geophys. Res., 97*, 10,103-10,108, 1992.

Minschwaner, K., R. J. Salawitch , and M. B. McElroy, Absorption of solar radiation by O_2: Implications for O_3 and lifetimes of N_2O, $CFCl_3$, and CF_2Cl_2, *J. Geophys. Res., 98*, 10,543-10,561, 1993.

Montzka, S. A., et al., Nitrous Oxide and Halocarbons Division, in *Climate Monitoring and Diagnostics Laboratory No. 20, Summary Report 1991*, edited by E. E. Ferguson and R. M. Rosson, NOAA Environmental Research Laboratories, Boulder, Colo., 1992.

Oltmans, S. J., Surface ozone measurements in clean air, *J. Geophys. Res., 86*, 1174-1180, 1981.

Pinnock, S, M. D. Hurley, K. P. Shine, T. J. Wallington, and T. J. Smyth, Radiative forcing of climate by hydrochlorofluorocarbons and hydrofluorocarbons, *J. Geophys. Res., 100*, 23,227-23,238, 1995.

Plumb, R. A., and M. K. W. Ko, Interrelationships between mixing ratios of long-lived stratospheric constituents, *J. Geophys. Res., 97*, 10,145-10,156, 1992.

Ramanathan, V., Greenhouse effect due to chlorofluorocarbons: Climatic implications, *Science, 190*,50-52, 1975.

Ramanathan, V., R. J. Cicerone, H. B Singh, and J. T. Keuhl, Trace gas trends and their potential role in climate change, *J. Geophys. Res., 90*, 5547-5566, 1985.

Ramanathan, V., L. Callis, R. Cess, J. Hansen, I. Isaksen, W. Kuhn, A. Lacis, F. Luther, R. Reck, and M. Schlesinger, Climate-chemical interactions and effects of changing atmospheric trace gases, *Rev. Geophys., 25*, 1441-1482, 1987.

Rossow, W. B., and R. A. Schiffer, ISCCP cloud data products, *Bull. Amer. Meteor. Soc., 72*, 2-20, 1991.

Roche, A. E., J. B. Kumer, J. L. Mergenthaler, G. A. Ely, W. G. Uplinger, J. F. Potter, T. C. James, and L. W. Sterritt, The Cryogenic Limb Array Spectrometer (CLAES) on UARS: experiment description and performance, *J. Geophys. Res., 98*, 10763-10776, 1993.

Rosenlof, K. H., and J. R. Holton, Estimates of the stratospheric residual circulation using the downward control principle, *J. Geophys. Res., 98*, 10,465-10,479, 1993.

Rottman, G. J., T. N. Woods, and T. P. Sparn, Solar-Stellar Irradiance Comparison Experiment 1, 1, instrument design and operation, *J. Geophys. Res., 98*, 10,667-10,678, 1993.

Stephens, G. L., Radiation profiles in extended water clouds, I: Theory, *J. Atmos. Sci., 35*, 2111-2122, 1978.

Stephens, G. L., and C. M. R. Platt, Aircraft observations of the radiative and microphysical properties of stratocumulus and cumulus cloud fields, *J. Clim. Appl. Meteorol., 26*, 1243-1269, 1987.

Tans, P. P., T. J. Conway, E. J. Dlugokencky, K. W. Thoning, P. M. Lang, K. A. Masarie, P. Novelli, and L. Waterman, Carbon Cycle Division, in *Climate Monitoring and Diagnostics Laboratory No. 20, Summary Report 1991*, edited by E. E. Ferguson and R. M. Rosson, NOAA Environmental Research Laboratories, Boulder, Colo., 1992.

Wang, W. C., Y. L. Yung, A. A. Lacis, T. Mo, and J. E. Hansen, Greenhouse effects due to man-made perturbations of trace gases, *Science, 194*, 685-690, 1976.

Wang, W. C., J. P. Pinto, and Y. L. Yung, Climatic effects due to halogenated compounds in the Earth's atmosphere, *J. Atmos. Sci., 37*, 333-338, 1980.

Water, J. W., Microwave limb sounding, *Atmospheric Remote Sensing by Microwave Radiometry*, M. A. Janssen, Ed., John Wiley and Sons, 383-496, 1993.

World Meteorological Organization), *Scientific Assessment of Ozone Depletion: 1991*, Global Ozone Research and Monitoring Project, Rep. No. 25, Geneva, 1991.

Woods, T. N., G. J. Rottman, and G. J. Ucker, Solar-Stellar Irradiance Comparison Experiment 1, 2, instrument calibrations, *J. Geophys. Res., 98*, 10,679-10,694, 1993.

Yoshino, K., A. S.-C. Cheung, J. R. Esmond, W. H. Parkinson, D. E. Freeman, and S. L. Guberman, Improved absorption cross sections of oxygen in the wavelength region 205-240 nm of the Herzberg continuum, *Planet. Space Sci., 36*, 1469-1475, 1988.

K. Minschwaner and R. W. Carver, Department of Physics, New Mexico Institute of Mining and Technology, Socorro, NM, 87801.

B. P. Briegleb, National Center for Atmospheric Research, Boulder, CO 80307.

This preprint was prepared with AGU's LaTeX macros v4. File forcing formatted January 12, 1998.

Figure 1. Distributions of CH_4 (upper left, in ppb), CCl_2F_2 (upper right, in ppt), N_2O (lower left, in ppb), and O_3 (lower right, in ppm) used in the radiative calculations for the September-October contemporary period.

Figure 2. Distributions of H_2O (upper left, volume mixing ratio), temperature (upper right, degrees Kelvin), and cloud fractions (lower center, percent) used in the radiative calculations for the September-October pre-industrial and contemporary time periods.

Figure 3. Top of atmosphere (TOA) infrared fluxes for June-July (3a) and December-January (3b). Diamonds indicate values calculated using the radiative model initialized with temperature, trace gas distributions, and clouds as described in the text. The solid curve bracketed by the ± 5 W/m^2 dotted curve indicates an average of 1985-88 observations from the Earth Radiation Budget Experiment.

Figure 4. Seasonal and latitudinal dependence of the post-industrial radiative forcing calculated for CH_4 (upper left), CCl_2F_2 (upper right), and N_2O (lower left). All forcings are in W m^{-2}. Also shown is the distribution of high cloud fraction used in the calculations (lower right).

Table 1. Forcing Results (W m^{-2})

Species	ΔF, Global Average	42°N Summer	*IPCC* [1995]
CH_4	0.536	0.564	0.47
CCl_2F_2	0.125	0.133	0.14
N_2O	0.108	0.112	0.14

Table 2. Forcing Sensitivities (%), Summer Season

Species	Clear Sky		Fix Strat	
	38°N	3°N	42°N	3°N
CH_4	+29	+36	+1	+1
CCl_2F_2	+36	+51	+8	+10
N_2O	+28	+35	+2	+1

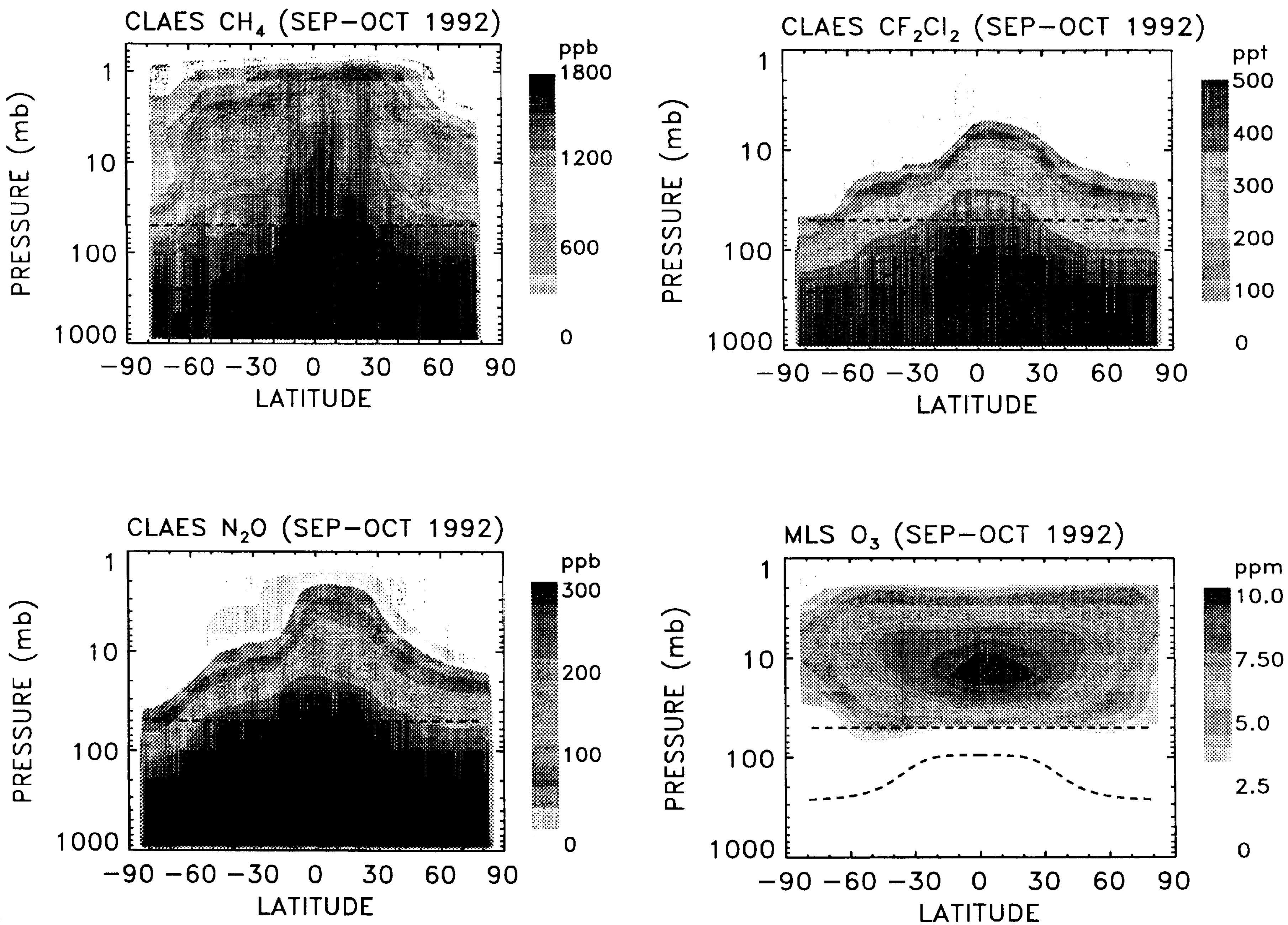
CLAES CH_4 (SEP–OCT 1992)
ppb
1800
1200
600
0
CLAES CF_2Cl_2 (SEP–OCT 1992)
ppt
500
400
300
200
100
0
CLAES N_2O (SEP–OCT 1992)
ppb
300
200
100
0
MLS O_3 (SEP–OCT 1992)
ppm
10.0
7.50
5.0
2.5
0
PRESSURE (mb)
1
10
100
1000
LATITUDE
−90 −60 −30 0 30 60 90

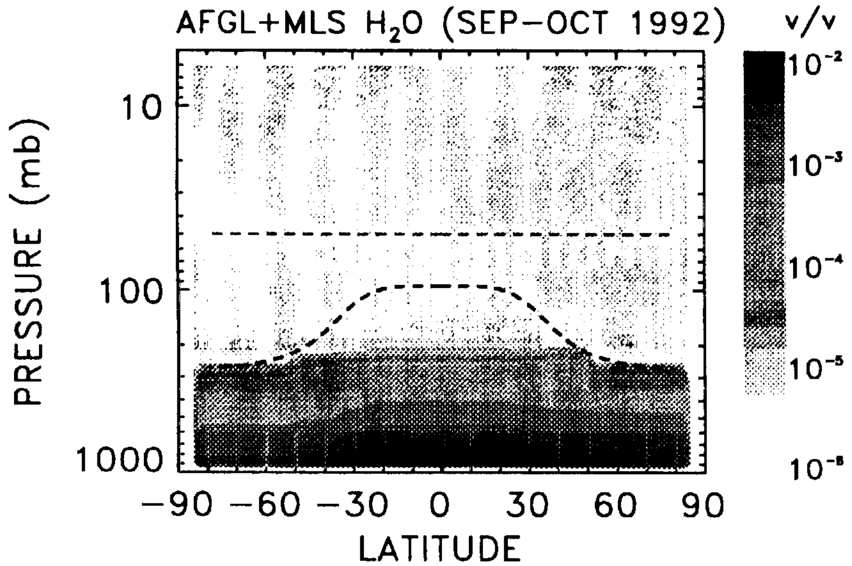
AFGL+MLS H_2O (SEP–OCT 1992)
PRESSURE (mb)
10
100
1000
LATITUDE
−90 −60 −30 0 30 60 90
v/v
10^{-2}
10^{-3}
10^{-4}
10^{-5}
10^{-6}

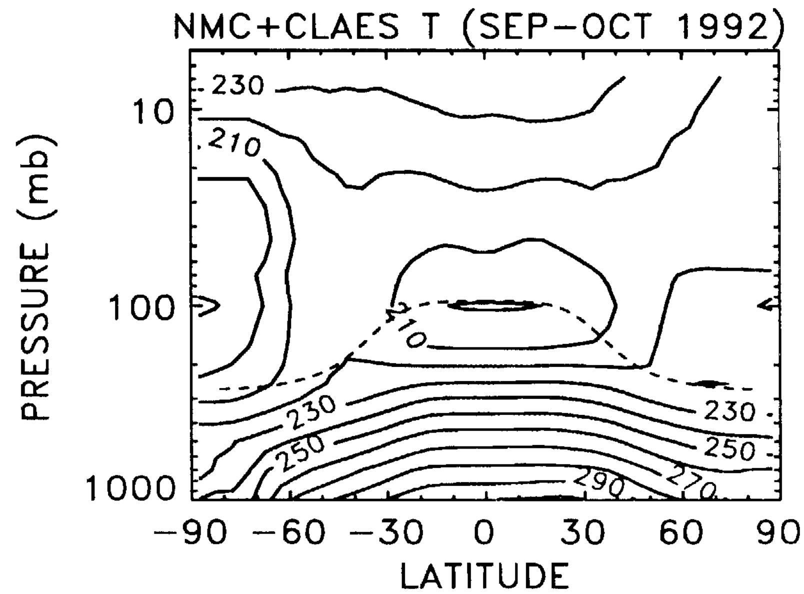
NMC+CLAES T (SEP–OCT 1992)
PRESSURE (mb)
10
100
1000
230
210
230
250
290
270
LATITUDE
−90 −60 −30 0 30 60 90

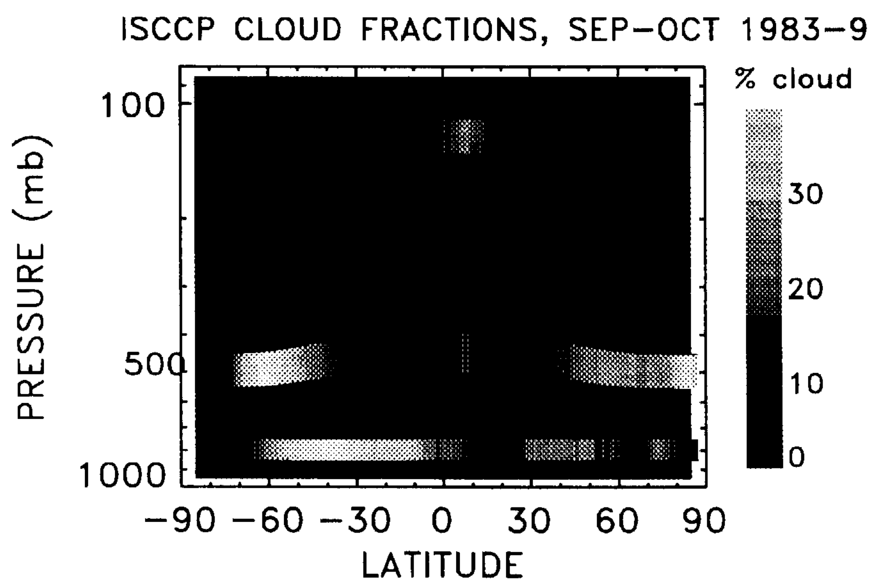
ISCCP CLOUD FRACTIONS, SEP–OCT 1983–90
PRESSURE (mb)
100
500
1000
LATITUDE
−90 −60 −30 0 30 60 90
% cloud
30
20
10
0

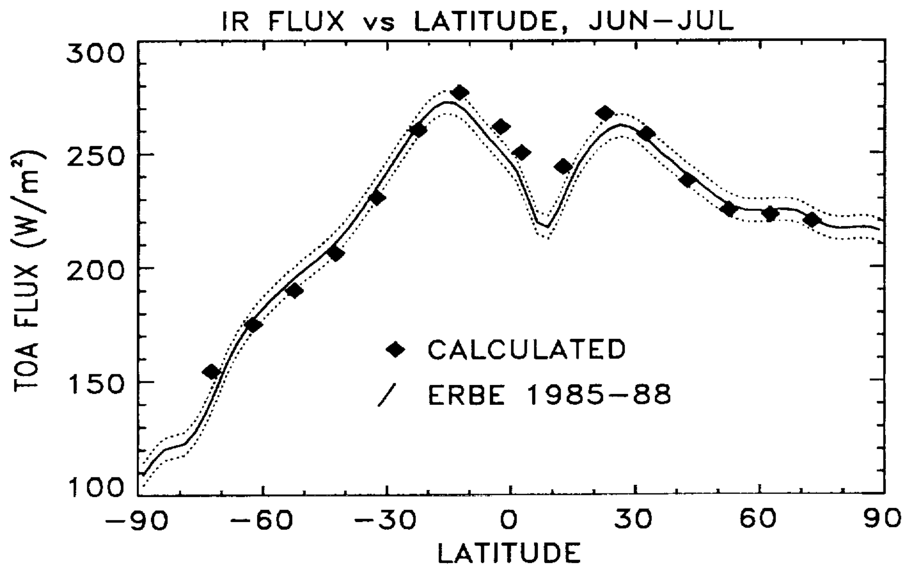
IR FLUX vs LATITUDE, JUN−JUL
TOA FLUX (W/m²)
300
250
200
150
100
−90
−60
−30
0
30
60
90
LATITUDE
CALCULATED
ERBE 1985−88

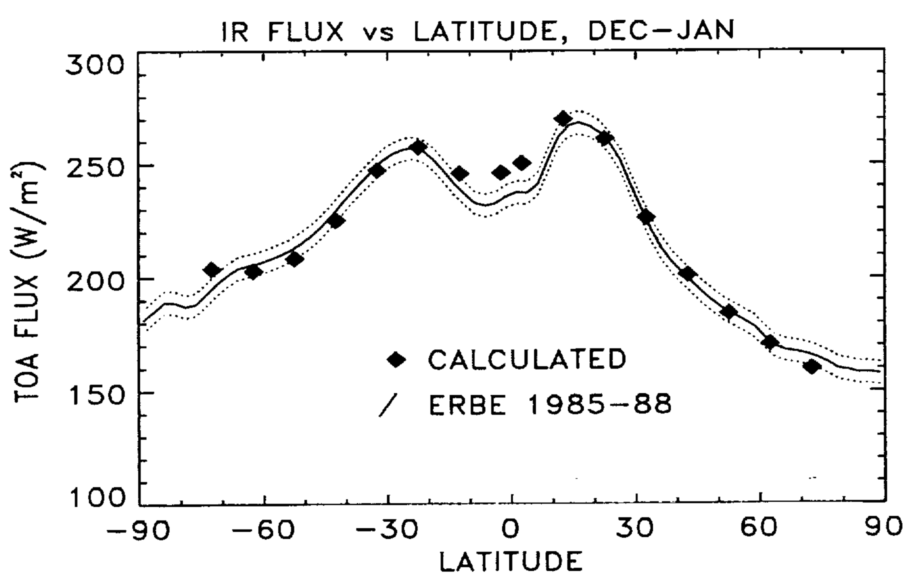
IR FLUX vs LATITUDE, DEC−JAN
TOA FLUX (W/m²)
300
250
200
150
100
−90
−60
−30
0
30
60
90
LATITUDE
CALCULATED
ERBE 1985−88

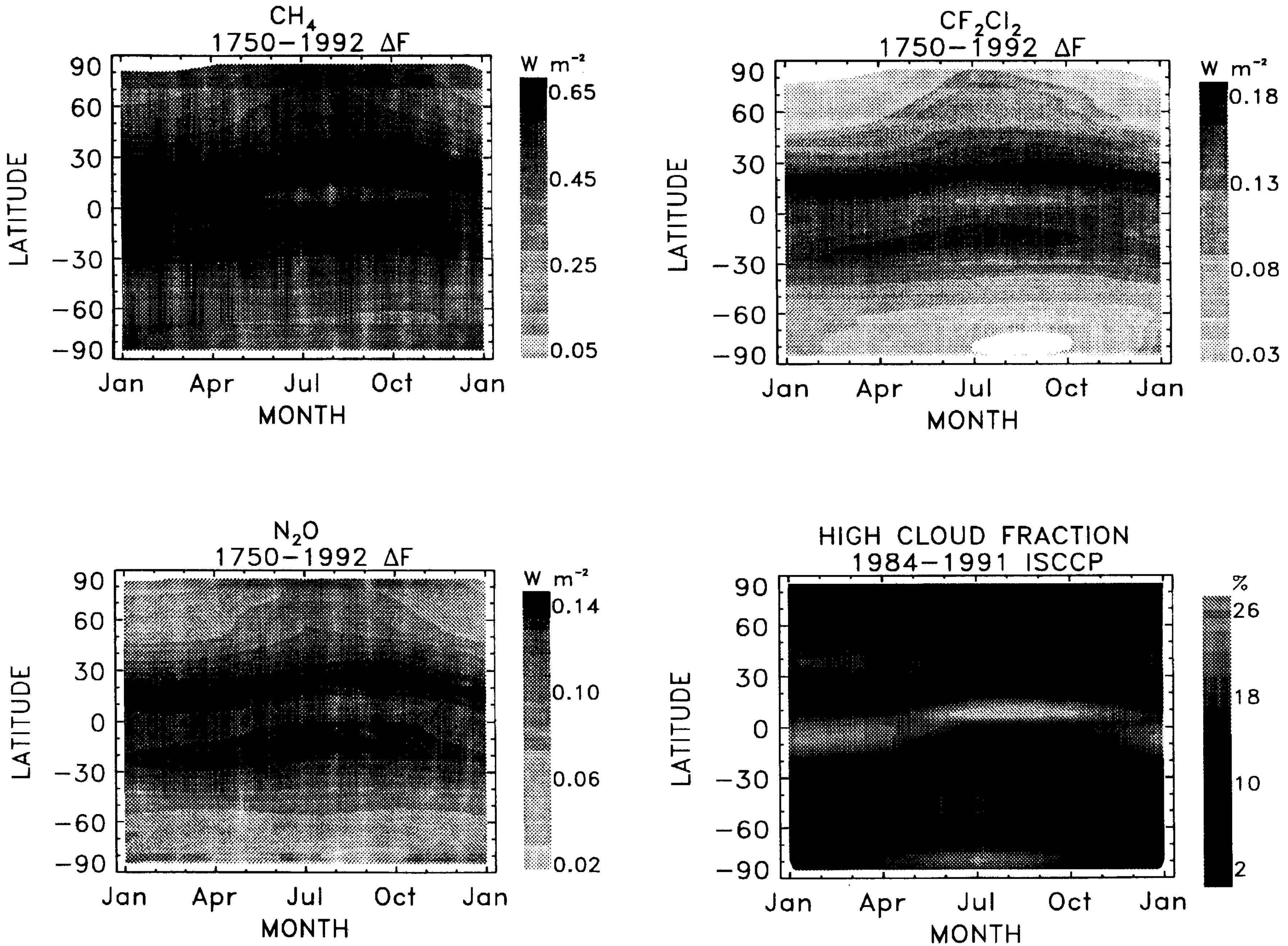
CH4
1750–1992 ΔF
W m⁻²
0.65
0.45
0.25
0.05
CF2Cl2
1750–1992 ΔF
W m⁻²
0.18
0.13
0.08
0.03
N2O
1750–1992 ΔF
W m⁻²
0.14
0.10
0.06
0.02
HIGH CLOUD FRACTION
1984–1991 ISCCP
%
26
18
10
2
LATITUDE
90
60
30
0
−30
−60
−90
Jan
Apr
Jul
Oct
Jan
MONTH